Video Article

Hemi-laryngeal Setup for Studying Vocal Fold Vibration in Three Dimensions

Christian T. Herbst[1,2], Vit Hampala[1], Maxime Garcia[2,3], Riccardo Hofer[2], Jan G. Svec[1]

[1]Voice Research Lab, Department of Biophysics, Faculty of Science, Palacky University Olomouc

[2]Laboratory of Bio-Acoustics, Dept. of Cognitive Biology, University of Vienna

[3]ENES Lab, NEURO-PSI,CNRS UMR 9197, Université Lyon/Saint-Etienne, France

Correspondence to: Christian T. Herbst at herbst@ccrma.stanford.edu

Abstract

The voice of humans and most non-human mammals is generated in the larynx through self-sustaining oscillation of the vocal folds. Direct visual documentation of vocal fold vibration is challenging, particularly in non-human mammals. As an alternative, excised larynx experiments provide the opportunity to investigate vocal fold vibration under controlled physiological and physical conditions. However, the use of a full larynx merely provides a top view of the vocal folds, excluding crucial portions of the oscillating structures from observation during their interaction with aerodynamic forces. This limitation can be overcome by utilizing a hemi-larynx setup where one half of the larynx is mid-sagittally removed, providing both a superior and a lateral view of the remaining vocal fold during self-sustained oscillation.

Here, a step-by-step guide for the anatomical preparation of hemi-laryngeal structures and their mounting on the laboratory bench is given. Exemplary phonation of the hemi-larynx preparation is documented with high-speed video data captured by two synchronized cameras (superior and lateral views), showing three-dimensional vocal fold motion and corresponding time-varying contact area. The documentation of the hemi-larynx setup in this publication will facilitate application and reliable repeatability in experimental research, providing voice scientists with the potential to better understand the biomechanics of voice production.

Video Link

The video component of this article can be found at https://www.jove.com/video/55303/

Introduction

Voice is typically created by vibrating laryngeal tissue (mainly the vocal folds), which converts a steady airflow, supplied by the lungs, into a sequence of airflow pulses. The acoustic pressure waveform (*i.e.*, the primary sound) emerging from this sequence of flow pulses acoustically excites the vocal tract which filters them, and the resulting sound is radiated from the mouth and (to a certain degree) from the nose[1]. The spectral composition of the generated sound is largely influenced by the quality of vocal fold vibration, governed by laryngeal biomechanics and interactions with the tracheal airflow[2]. Both in a clinical and a research context, documentation and assessment of vocal fold vibration is thus of foremost interest when studying voice production.

In humans, direct endoscopic investigation of the larynx during sound production *in vivo* is challenging, and it is virtually impossible in nonhuman mammals, given current technological means. Therefore, and in order to guarantee carefully controlled physical and/or physiological experimental boundary conditions, the use of excised larynges[3,4] is in many cases an adequate substitution for investigation of *in vivo* voice production mechanisms.

Vocal fold vibration is a complex three-dimensional phenomenon[5]. While conventional investigation methods like laryngeal endoscopy (*in vivo*) or excised larynx preparations typically provide only a superior view of the vibrating vocal folds[6], they do not allow for complete three-dimensional analysis of vocal fold motion. In particular, in the superior view the lower (caudal) margins of the vocal folds are invisible during a major portion of the vibratory cycle. This is due to the phase delay between the inferior (caudal) and the superior (cranial) edge of the vocal folds, a phenomenon which is typically seen during vocal fold oscillation[5]. As direct empirical evidence for backing up findings from mathematical and physical models is scarce, knowledge of the geometry and motion of the lower vocal fold edge[7], and thus the geometry of the subglottal channel[8,9,10] is crucial for better understanding the interaction between laryngeal airflow, vocal fold tissue, and the resulting forces and pressures[11,12]. Another aspect of vocal fold vibration that is hidden from the customary superior view is the vertical (caudo-cranial) depth of the contact between the two vocal folds. The vertical contact depth is related to the vertical thickness of the vocal folds, which is a potential indicator of the vocal register used in singing ("chest" vs. "falsetto" register)[13,14].

In order to overcome the shortcomings of conventional (full) excised larynx preparations, a so-called hemi-larynx setup can be utilized, where one half of the larynx is removed, thus facilitating the assessment of the vibratory characteristics of the remaining vocal fold in three dimensions. Surprisingly, since the introduction of this setup in the 1960s[15] and an initial validation of the concept in 1993[16], not many laboratories have

performed experiments with this promising experimental approach[17,18,19,20,21,22,23]. An explanation for this might be found in the difficulties of creating a viable hemi-larynx preparation. While the conventional excised (full) larynx preparation is well documented[4], no such in-depth instructions are as yet available for creating a hemi-larynx setup. It is therefore the purpose of this paper to provide a tutorial for establishing a reliably reproducible hemi-larynx setup, supplemented by experimental results from red deer specimens.

A hemi-larynx setup shares many features with a "conventional" excised larynx setup, such as measurement equipment, high-speed or other imaging technology to adequately document the vibrations of the laryngeal structures during sound generation, or proper supply of heated, humidified air. These general setup considerations are described in detail in both a book chapter[4] and a technical report from the National Center of Voice and Speech[24]. Reiteration of these instructions would be beyond the scope of this manuscript. Here, only the specialized directives for generating a hemi-larynx setup are presented.

Protocol

The animal specimens analyzed in this paper were treated in accordance with the standard ethical requirements of the Palacky University in Olomouc, Czech Republic. They stem from red deer living wildly in forests, which were hunted by the Czech Army Forest Service during a regular hunting season.

1. Preparation of the Hemi-larynx Specimen

Note: Only properly prepared specimens should be used, as indicated in[4]. Quick freezing of the larynx[25] immediately after excision and storage at -80 °C minimizes the potential of tissue degradation and alteration of biomechanical properties, and allows performing the experiments at any convenient time.

1. **Defrosting the larynx**
   1. Insert the frozen larynx into two autoclave bags or any other plastic bags with waterproof sealing. Seal the bags and put them into a water bath heated to 30 °C until the larynx is completely defrosted. The duration required ranges from a few hours to more than a day, depending on larynx size and freezing temperature.

2. **Cleaning the larynx**
   1. After the larynx is defrosted, remove it from the bag and clean it thoroughly with saline solution (0.9% NaCl).
   2. Carefully remove superfluous tissue as applicable (i.e. external neck muscles, hyoid bone etc.) without damaging the main laryngeal structures, and shorten the trachea to a length adequate for mounting the larynx onto an air supply tube (usually ca. 4-5 cm).
   3. Check the laryngeal tissue for potential tissue anomalies, such as wounds, organic deformations, or cracks potentially occurring from the freezing process, which could make the larynx unsuitable for the experiment.

3. **Exposure of the thyroid and cricoid cartilages**
   1. Remove parts of the external laryngeal muscle tissue around the thyroid and cricoid cartilage using a scalpel, thus exposing the cartilages in preparation for the mid-sagittal cut creating the hemi-larynx. This preparation stage is depicted in **Figure 1A** and **1B**.

4. **Mid-sagittal cut through the thyroid cartilage**
   1. Make an initial vertical cut through the anterior part of the thyroid cartilage.
   2. Carefully place the cut slightly more onto the side that is about to be removed, in order not to damage the vocal fold that needs to remain preserved. If possible, use a scalpel for cutting. If the cartilage is ossified, use a small saw.

5. **Cutting the cricoid cartilage**
   1. Lead the cut vertically (inferiorly) from in between the arytenoid cartilages and then through the cricoid cartilage to an approximately horizontal level of the inferior thyroid notch.

6. **Removal of one vocal fold, creating an L-shaped incision in the larynx**
   1. Make a horizontal cut starting from the inferior end of the previously made vertical cut in the cricoid cartilage, and lead the new cut towards the inferior thyroid notch. Anteriorly fold the side of the larynx that is going to be removed.
   2. Make a vertical cut through the soft tissue on the inner side of the thyroid cartilage - be careful while leading the cut in between the anterior attachment of the vocal folds to the thyroid cartilage, thus avoiding damage to the vocal fold.

7. **Refinement of the cut through the thyroid cartilage**
   1. Use a scalpel, a saw, or a file, in order to apply a precisely straight cut in the thyroid cartilage, and get as close as possible to the anterior part of the previously inspected vocal fold.
   2. Remove also a small part of the posterior thyroid cartilage, in order to create space for inserting the prong for adducting the arytenoid cartilage and thus the vocal fold (see below). This preparation stage is depicted in **Figure 1C** and **1D**.
   Note: Depending on the research question, full exposition of the whole vocal fold may be needed to enable its visibility from above. In such a case, the structures above the (true) vocal fold (i.e., the ventricular or vestibular fold, as applicable given the anatomy of the specimen) should be removed. In some specimens the inner soft laryngeal tissue above the vocal folds might lose its connection with the thyroid cartilage and interferes with the vocal fold during vibration, potentially causing spurious (mostly irregular) oscillatory patterns. In such a case careful removal of that tissue is inevitable.
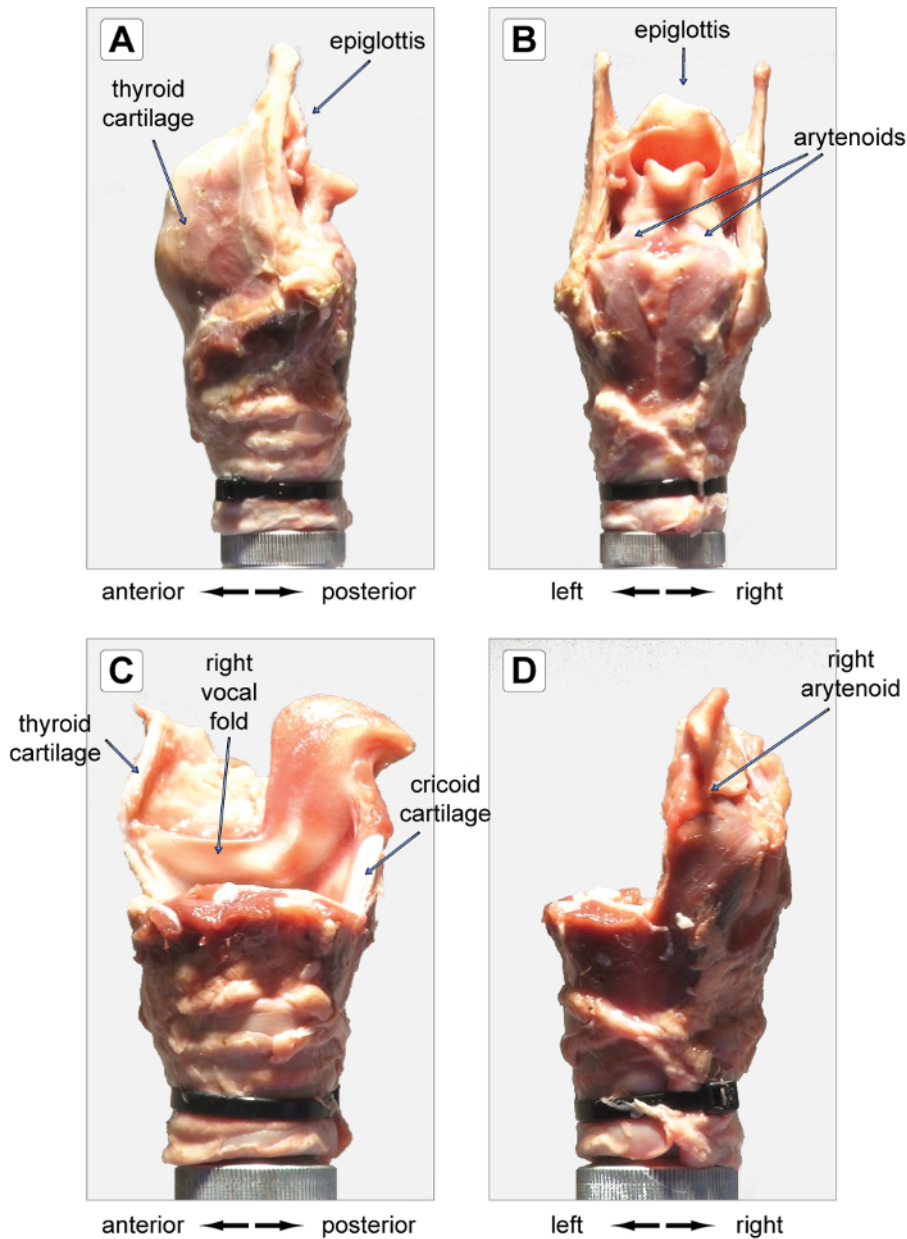
Figure 1: Hemi-larynx preparation and mounting. (**A**) and (**B**) Cleaned larynx specimen, medial and posterior view, before removal of left vocal fold; (**C**) and (**D**) Prepared hemi-larynx with L-shaped incision (left vocal fold removed), medial and posterior view. Please click here to view a larger version of this figure.

2. Hemi-larynx Experiment

1. **Hemi-laryngeal setup**
    1. Use an air-supply tube which delivers warmed and humidified air into the larynx.
    2. Construct two perpendicularly arranged transparent plates as a substitution for removed laryngeal parts.
    3. Use prongs [4] for increasing the stability of the larynx and creating a proper pre-phonatory larynx configuration by adducting the remaining vocal fold to the vertical glass plate (see **Figure 2A**).
    Note: Theoretically, the vocal folds might also be adducted by sutures and weights on a pulley-lever system [26]. However, such an approach has, to the best knowledge of these authors, not yet been attempted for a hemilarynx preparation.
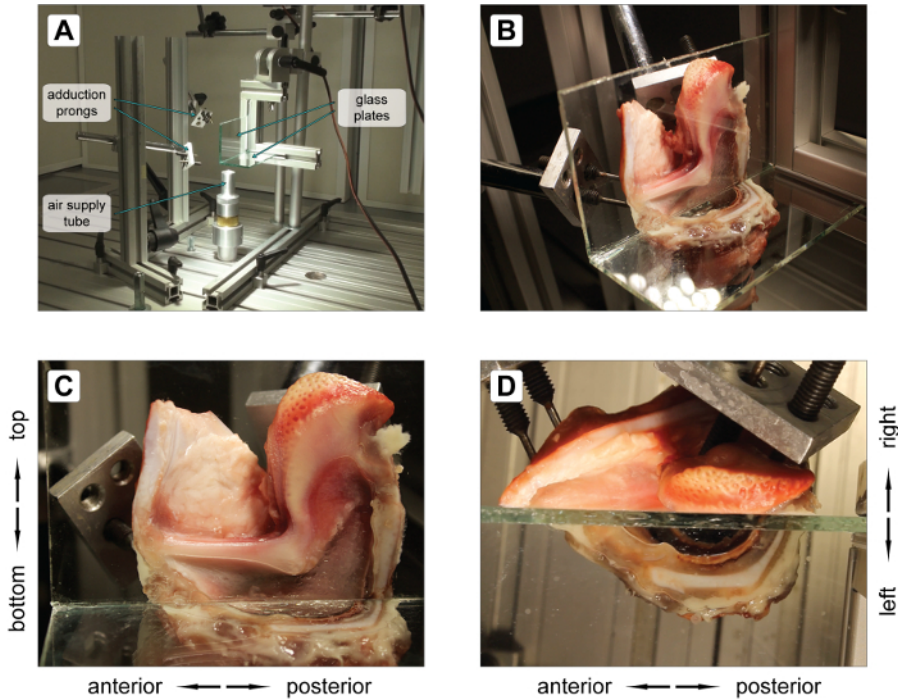
Figure 2: Hemi-larynx setup. (**A**) Supporting structures: air supply tube, L-shaped glass plate arrangement, adduction prongs. (**B**) Mounted hemi-larynx preparation with adduction prongs. (**C**) and (**D**) Close-ups of hemi-larynx-preparation, viewed from the side and from the top, respectively. Please click here to view a larger version of this figure.

2. **Mounting the hemi-larynx**
   1. Cover the air supply tube with denture fixative cream and mount the larynx using the remaining part of its trachea. The fixative cream works as an adhesive and closes potential gaps, thus creating an air-tight seal.
   2. Fasten the trachea with a plastic tightening strap or a hose clamp.
   3. Also cover the edges of the cut through the thyroid cartilage with the fixative cream, while avoiding spreading fixative cream on the vocal fold or the inner soft laryngeal tissues.
   4. Attach the transparent plates.

3. **Stabilization of the thyroid cartilage, adduction of the vocal fold using prongs**
   1. Use the prongs to adduct the vocal fold to the plate and stabilize the thyroid cartilage.
   2. After the fixative cream has set, apply the airflow in order to establish vocal fold oscillation and check for possible leaks between the hemi-larynx and the glass plates.
   3. Seal eventually occurring gaps by adding more fixative cream.

Representative Results

Illustrations of the hemi-larynx preparation and its mounting on the air supply tube, as referenced in the previous section, are provided in **Figure 1** and **Figure 2**, respectively.

Documentation of vocal fold vibration from two camera angles

Airflow-induced self-sustaining oscillation of the hemi-larynx vocal fold was documented from the top and from the side with two synchronized high-speed video (HSV) cameras operated at 6,000 frame/s, complemented by time-synchronous recordings of acoustic and electroglottographic (see below) data sampled at 44.1 kHz. More information on the data acquisition setup including a list of equipment used can be found in previous publications by this group of authors [27,28]. Footage from these HSV recordings is shown in the accompanying video. Still images, extracted at representative moments within the vibratory cycle, are shown in **Figure 3**. The top view (upper half of each panel) shows medio-lateral vocal fold movement, indicating an open glottis in **Figure 3A**, allowing glottal air flow, whilst in **Figure 3B-D** the glottis is closed (the vocal fold is in complete contact with the vertical glass plate), thus arresting the glottal air flow. The side view (lower half of each panel) in **Figures 3B-D** suggests a varying degree of vocal fold contact against the glass plate, as well as a varying geometry and vertical location of that contact.
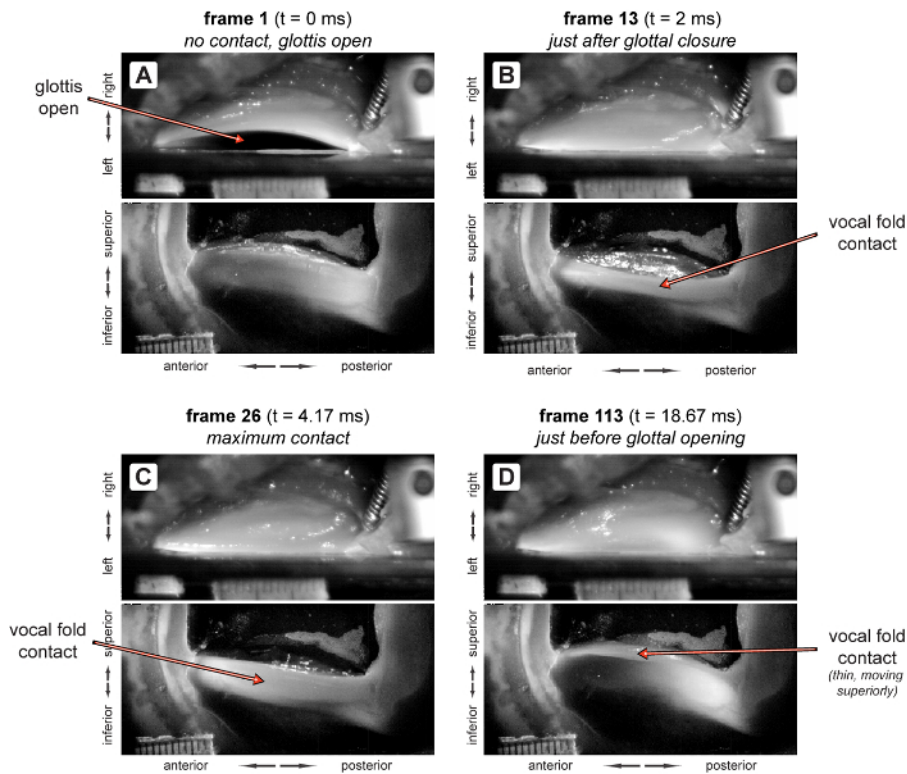
Figure 3: Hemi-larynx vocal fold vibration. (**A-D**) Still images from high-speed video footage from the top (upper half of each panel) and the side view cameras (lower half of each panel), extracted at representative points within the vibratory cycle. Note the absence of vocal fold contact in (A), and the varying (both in area, shape, and position) vocal fold contact in (**B-D**). Please click here to view a larger version of this figure.

Kymographic glottal motion analysis

Quantitative glottal motion analysis is illustrated in **Figure 4**. The glottis is the variable opening between the (vibrating) vocal folds[29], created by their deflections during self-sustained oscillation. State of the art analysis of top view HSV footage allows tracing the lateral deflections of the vocal folds[30,31]. The hemi-larynx preparation described here adds the facility to assess also the vertical (caudo-cranial) aspects of vocal fold vibration.
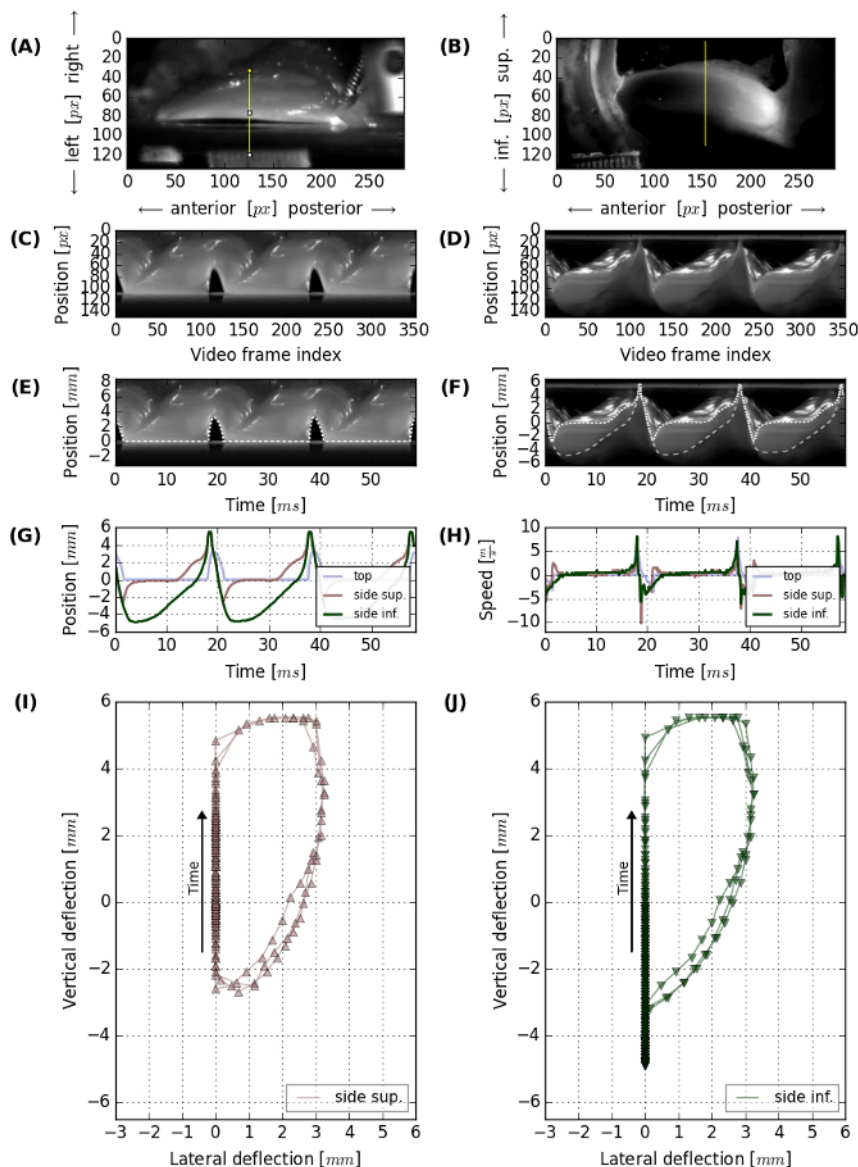
Figure 4: Kymographic glottal motion analysis.
(**A**) and (**B**) Video stills showing top and side views of the hemi-larynx, taken from high-speed video (HSV) recordings at 6,000 frames/s. The yellow vertical lines indicate the kymographic scan line position for the kymograms shown in panels C and E for the top view, and panels D and F for the side view. (**C**) and (**D**) Digital kymograms extracted from the HSV footage of the top and the side view, respectively. (**E**) The time-varying lateral displacement of the vocal fold extracted from the kymogram and traced with a line (short dashes). (**F**) The time-varying deflections of the inferior and superior edges of the vocal fold, assessed from the kymogram and traced with a dashed and a dotted line, respectively. (**G**) Synoptic depiction of the time-varying glottal structures: Lateral vocal fold deflection ("top", pale violet), and vertical deflection of the superior ("side sup.", dark red) and inferior ("side inf.", dark green) vocal fold edges extracted from the kymograms shown in panels E and F. (**H**) Motion speeds derived from the glottal structure displacement data shown in panel G. (**I**) and (**J**) Glottal motion reconstruction derived from the displacement data of the superior and inferior vocal fold margins shown in panel G. The arrows indicate the direction of the rotational movement. Please click here to view a larger version of this figure.

Two digital kymograms were generated from top and side view HSV data (Figures 4C and 4D). In a digital kymogram (DKG)[32,33,34,35], the pixel data from a single line (typically at the point of maximum vocal fold vibratory amplitude), taken from a number of consecutive high-speed video frames, are concatenated to form a temporal axis on the abscissa. The time-varying displacement of the structures covered by the DKG scan line is visible on the ordinate. In the example shown in **Figure 4C**-**F**, the DKG scan line positions of the top and side view were selected halfway along the antero-posterior (ventro-dorsal) dimension of the vocal fold, utilizing the approach described by Hampala *et al*., Eq. 1[27].

The lateral and caudo-cranial deflections of the glottis, delineated by the inferior and superior vocal fold edges, were traced within the DKG data (Figures 4E and 4F) and expressed in metric units based on the video frame rate and calibration information embedded in the videos (**Figure 4G** and **H**). A reconstruction of the two-dimensional (lateral and vertical) glottal motion at the middle of the vocal fold (i.e., the place of maximum vibratory amplitude) over three complete glottal cycles is shown in **Figure 4E** and **F**. During the majority of the glottal cycle, the vocal fold was in contact with the glass plate (representing glottal closure), but with varying contact depth. During the open phase (*i.e.*, when the vocal fold is not in contact with the glass plate), the traces of the inferior and the superior vocal fold edge fuse, and they exhibit a complex cyclic motion pattern, in partial agreement with results from other studies [5,20,36,37] (the motion pattern found in humans tends to be more elliptical than that of the red deer specimen investigated here). Interestingly, the vertical displacement reached a vibratory amplitude of about 10 mm, *i.e.*, almost an order of magnitude larger than what was found in humans.

Assessment of vocal fold contact area

Electroglottography (EGG)[38] is a widely used non-invasive method for measuring changes in relative vocal fold contact area (VFCA) during phonation. A low intensity, high-frequency current is passed between two electrodes placed at vocal fold level on each side of the larynx. The admittance variations resulting from vocal fold (de)contacting during laryngeal sound production are largely proportional to the time-varying relative vocal fold contact area[39]. The EGG signal is assumed to be a reliable physiological correlate of vocal fold vibration, reflecting the fundamental frequency and the oscillatory regime (irregular or periodic, including bifurcations). Despite its broad application, the possible direct relation between the VFCA and the EGG waveform has, until recently, only been tested in a single study[17], suggesting an approximately linear relationship between VFCA and the EGG signal magnitude. However, flow-induced vocal fold vibration was not investigated in that study. Therefore, a rigorous empirical evaluation of EGG as a measure of relative VFCA under proper physiological conditions was therefore still needed.

In addressing this issue, this group of authors has recently investigated three red deer larynges in an excised hemi-larynx preparation utilizing a conducting glass plate[27]. The time varying contact between the vocal fold and the glass plate was monitored by high-speed video recordings made in the sagittal plane at 6000 fps, synchronized with the EGG signal with an accuracy of ± 0.167 ms. Representative results from that study are shown in **Figure 5**, indicating an average to good agreement between the EGG signal and VFCA – see reference[27] for details).
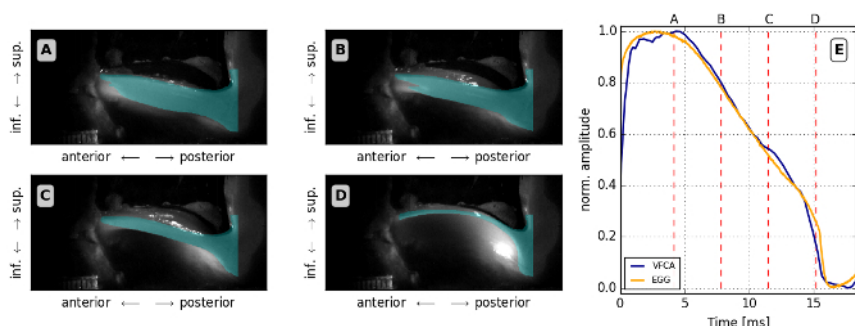

Figure 5: Comparison of vocal fold contact area (VFCA) and electroglottographic (EGG) waveform. (**A-D**) Video stills from high-speed video data showing the side view of a red deer hemi-larynx at four instants within a glottal cycle. The manually assessed vocal fold contact area (*i.e.*, the area where the vocal fold was in contact with the vertical glass plate in the hemi-larynx setup) is superimposed in cyan. (**E**) Comparison of normalized EGG and VFCA data for the vocal fold contact phase of one glottal cycle. The VFCA data stemmed from assessment of vocal fold contact area (counted in pixels) over the glottal cycle. Please click here to view a larger version of this figure.

Discussion

The hemi-larynx preparation shares the advantages of the "conventional" (full) excised larynx setup: In such an experimental approach, physical and physiological boundary conditions and parameters (such as subglottal pressure or vocal fold elongation) can be controlled fairly well. The behavior of the hemilarynx is homologous to that of a full larynx with a perfect lateral symmetry, with the exception that magnitudes of some parameters (*e.g.*, air flow rate, sound pressure) are reduced by approximately 50 %, yet still being within realistic ranges[16]. The major disadvantage of the full excised larynx approach, *i.e.*, the lack of visibility of the vocal fold surface along the superior-inferior (caudo-cranial) dimension, is overcome in the hemi-larynx setup by providing a side view of the vibrating vocal fold. The hemi-larynx setup thus allows assessment of vocal fold motion in multiple dimensions, which is crucial when trying to understand the finer details of the biophysical sound generation mechanism in humans and nonhuman mammals.

Here, several exemplary applications of the hemi-larynx setup have been demonstrated. The documentation of vocal fold vibration from two camera angles allows further qualitative and quantitative data analysis. The kymographic glottal motion analysis in the vertical direction, newly introduced in this paper, allows reconstruction of the temporal geometric variations of the glottis along a selected position along the antero-posterior (dorso-ventral) glottal axis. When repeating this analysis for several points equidistantly spaced along the glottal axis, the entire glottal motion could be reconstructed. Note that this approach provides comparable but not identical results as compared to assessment of vocal fold motion by marking and tracking individual "fleshpoints" in the vocal fold tissue (also on points not forming the glottis), *e.g.*, with micro-sutures[20] or silicon carbide particles[5,40]. Precise knowledge about the time-varying glottal geometry in three dimensions is crucial to further investigate details of the glottal airflow and its interaction with the vibrating laryngeal tissue. For example, computational models of self-sustaining vocal fold vibration could be improved as more empirical data concerning the point of airflow jet separation [41,42,43,44,45,46,47,48] become available.

As illustrated in **Figure 5**, the hemi-larynx preparation enables assessment of the vocal fold contact area (VFCA) during self-sustained vocal fold vibration. For one, knowledge of the time-varying relative magnitude of VFCA is useful to validate the results from electroglottographic

measurements[27], as EGG is a widely-used method for non-invasive assessment of vocal fold vibration *in vivo*. Furthermore, measurement of the exact VFCA geometry and its variation over time might prove to be crucial for better understanding the notion of vocal fold contact depth [49] and its potential relation to the speed of the so-called mucosal wave[50,51,52,53]. There, an airflow-driven travelling wave occurs within the surface cover layer of the vocal fold tissue. This wave moves initially along with the trans-glottal airflow from the inferior to the superior vocal fold edge, and then it propagates laterally across the upper vocal fold surface once every oscillatory cycle[54].

All things considered, the hemi-larynx approach is a powerful, yet not widely used constituent of the currently available arsenal of empirical methods for basic voice science. Here, a tutorial for creating a hemi-larynx preparation is presented, and some potential future applications are discussed. The given instructions may help improving the repeatability of experiments across different labs, thus providing voice scientists with the potential to better understand the biomechanics of voice production.

Disclosures

The authors have nothing to disclose.

Acknowledgements

References

1. Story, B.H. An overview of the physiology, physics and modeling of the sound source for vowels. *Acoust Sci Technol.* **23** (4), 195-206 (2002).
2. Titze, I.R. *Principles of voice production (second printing).* National Center for Voice and Speech, Iowa City, IA (2000).
3. Cooper, D.S. Research in laryngeal physiology with excised larynges. In: *Otolaryngology - head and neck surgery.* Vol. 3, Cummings, C.W., Fredrickson, J.M., Harker, L.A., Schuller, D.E., & Krause, C.J. eds., Ch. 95, C. V. Mosby, St. Louis and Toronto, 1728-1737 (1986).
4. Titze, I.R. Experiments with excised larynges. In: *The myoelastic aerodynamic theory of phonation.* Titze, I.R. ed., National Center for Voice and Speech, Denver CO and Iowa City IA, 1-62 (2006).
5. Baer, T. *Investigation of phonation using excised larynxes. (Doctoral dissertation).* Massachusetts Institute of Technology, Cambridge, Mass (1975).
6. Bless, D.M., Patel, R.R., & Connor, N. In: *The Larynx. Third Edition. Volume I.* Fried, M.P., & Ferlito, A. eds., Ch. 11, Plural Publishing, San Diego, CA, 181-210 (2009).
7. Berke, G.S. *et al.* Laryngeal modeling: theoretical, in vitro, in vivo. *Laryngoscope.* **97** 871-881 (1987).
8. Scherer, R.C., Titze, I.R., & Curtis, J.F. Pressure-flow relationships in two models of the larynx having rectangular glottal shapes. *J Acoust Soc Am.* **73** (2), 668-676 (1983).
9. Sidlof, P. *et al.* Geometry of human vocal folds and glottal channel for mathematical and biomechanical modeling of voice production. *J Biomech.* **41** (5), 985-995 (2008).
10. Scherer, R.C., Torkaman, S., Kuehn, D.P., & Afjeh, A.A. Intraglottal pressures in a three-dimensional model with a non-rectangular glottal shape. *J Acoust Soc Am.* **128** (2), 828-838 (2010).
11. Titze, I.R. The physics of small-amplitude oscillation of the vocal folds. *J Acoust Soc Am.* **83** (4), 1536-1552 (1988).
12. Horacek, J., & Svec, J.G. Instability boundaries of a vocal fold modelled as a flexibly supported rigid body vibrating in a channel conveying fluid. In: *Proceedings of the 5th International Symposium on Fluid Structure Interaction, Aeroelasticity, Flow Induced Vibration and Noise (IMECE2002), Vol.3 ASME Int. Mechanical Engineering Congress, 17-22 November 2002, New Orleans, Louisiana, USA (CD-ROM).* Paidoussis, M.P. ed., Ch. 2, American Society of Mechanical Engineers (ASME), New York, NY, USA, 1043-1054 (2002).
13. Vilkman, E., Alku, P., & Laukkanen, A.-M. Vocal-fold collision mass as a differentiator between registers in the low-pitch range. *J Voice.* **9** (1), 66-73 (1995).
14. Herbst, C.T., & Svec, J.G. Adjustment of glottal configurations in singing. J *Singing.* **70** (3), 301-308 (2014).
15. Hiroto, I. *Vibration of vocal cords: an ultra high-speed cinematographic study. (Film).* Department of otolaryngology, Kurume University, Kurume, Japan (1968).
16. Jiang, J.J., & Titze, I.R. A methodological study of hemilaryngeal phonation. *Laryngoscope.* **103** (8), 872-882 (1993).
17. Scherer, R.C., Druker, D.G., & Titze, I.R. In: *Vocal physiology: voice production, mechanisms and functions.* Fujimura, O. ed., Raven Press, New York, 279-291 (1988).
18. Jiang, J.J., & Titze, I.R. Measurement of vocal fold intraglottal pressure and impact stress. *J Voice.* **8** (2), 132-144 (1994).
19. Alipour, F., & Scherer, R.C. Dynamic glottal pressures in an excised hemilarynx model. *J Voice.* **14** (4), 443-454 (2000).
20. Berry, D.A., Montequin, D.W., & Tayama, N. High-speed digital imaging of the medial surface of the vocal folds. *J Acoust Soc Am.* **110** (5, Pt.1), 2539-2547 (2001).
21. Döllinger, M., Tayama, N., & Berry, D.A. Empirical eigenfunctions and medial surface dynamics of a human vocal fold. *Methods Inf Med.* **44** (3), 384-391 (2005).
22. Döllinger, M., Berry, D.A., & Berke, G.S. Medial surface dynamics of an in vivo canine vocal fold during phonation. *J Acoust Soc Am.* **117** (5), 3174-3183 (2005).
23. Döllinger, M., Berry, D.A., & Kniesburges, S. Dynamic vocal fold parameters with changing adduction in ex-vivo hemilarynx experiments. *J Acoust Soc Am.* **139** (5), 2372-2385 (2016).
24. Durham, P.L., Scherer, R.C., Druker, D.G., & Titze, I.R. *Development of excised larynx procedures for studying mechanisms of phonation. Technical report.* Voice Acoustics and Biomechanics Laboratory, Department of Speech Pathology and Audiology, The University of Iowa (1987).

25. Chan, R.W., & Titze, I.R. Effect of postmortem changes and freezing on the viscoelastic properties of vocal fold tissues. *Ann Biomed Eng.* **31** (4), 482-491 (2003).
26. Berg van den, Jw., & Tan, T.S. Results of experiments with human larynxes. *Practica Oto-Rhino-Laryngologica.* **21** 425-450 (1959).
27. Hampala, V., Garcia, M., Svec, J.G., Scherer, R.C., & Herbst, C.T. Relationship between the electroglottographic signal and vocal fold contact area. *J Voice.* **30** (2), 161-171 (2016).
28. Herbst, C.T. *et al.* Glottal opening and closing events investigated by electroglottography and super-high-speed video recordings. *J Exp Biol.* **217** (6), 955-963 (2014).
29. Zemlin, W.R. *Speech and hearing science: Anatomy & physiology.* 3 edn., Prentice Hall, New Jersey (1988).
30. Lohscheller, J., Toy, H., Rosanowski, F., Eysholdt, U., & Döllinger, M. Clinically evaluated procedure for the reconstruction of vocal fold vibrations from endoscopic digital high-speed videos. *Med. Image Anal.* **11** (4), 400-413 (2007).
31. Wittenberg, T., Moser, M., Tigges, M., & Eysholdt, U. Recording, processing, and analysis of digital high-speed sequences in glottography. *Mach Vis Appl.* **8** (6), 399-404 (1995).
32. Larsson, H., Hertegard, S., Lindestad, P.A., & Hammarberg, B. Vocal fold vibrations: high-speed imaging, kymography, and acoustic analysis: a preliminary report. *Laryngoscope.* **110** (12), 2117-2122 (2000).
33. Wittenberg, T., Tigges, M., Mergell, P., & Eysholdt, U. Functional imaging of vocal fold vibration: digital multislice high-speed kymography. *J Voice.* **14** (3), 422-442 (2000).
34. Deliyski, D., & Petrushev, P. In: *AQL 2003 Hamburg: Proceeding Papers for the Conference Advances in Quantitative Laryngology, Voice and Speech Research. (CD ROM).* Schade, G., Müller, F., Wittenberg, T., & Hess, M. eds., IRB Verlag, Stuttgart, Germany, 1-16 (2003).
35. Svec, J.G., & Schutte, H.K. Kymographic imaging of laryngeal vibrations. *Curr Opin Otolaryngol Head Neck Surg.* **20** (6), 458-465 (2012).
36. Doellinger, M., & Berry, D.A. Visualization and quantification of the medial surface dynamics of an excised human vocal fold during phonation. *J Voice.* **20** (3), 401-413 (2006).
37. Kusuyama, T., Fukuda, H., Shiotani, A., Nakagawa, H., & Kanzaki, J. Analysis of vocal fold vibration by x-ray stroboscopy with multiple markers. *Otolaryngol Head Neck Surg.* **124** (3), 317-322 (2001).
38. Fabre, P. Un procédé électrique percutané d'inscription de l'accolement glottique au cours de la phonation: glottographie de haute fréquence; premiers résultats. [A non-invasive electric method for measuring glottal closure during phonation: High frequency glottography: first results]. *Bull. Acad. Nat. Méd.* **141** 66-69 (1957).
39. Baken, R.J. Electroglottography. *J Voice.* **6** (2), 98-110 (1992).
40. Baer, T. In: *Vocal Fold Physiology.* Stevens, K.N., & Hirano, M. eds., University of Tokyo Press, Tokyo, 119-133 (1981).
41. Pelorson, X., Hirschberg, A., van Hassel, R.R., Wijnands, A.P.J., & Auregan, Y. Theoretical and experimental study of quasisteady-flow separation within the glottis during phonation. Application to a modified two-mass model. *J Acoust Soc Am.* **96** (6), 3416-3431 (1994).
42. Alipour, F., & Scherer, R.C. Flow separation in a computational oscillating vocal fold model. *J Acoust Soc Am.* **116** (3), 1710-1719 (2004).
43. Zhang, Z. Influence of flow separation location on phonation onset. *J Acoust Soc Am.* **124** (3), 1689-1694 (2008).
44. Kaburagi, T., & Tanabe, Y. Low-dimensional models of the glottal flow incorporating viscous-inviscid interaction. *J Acoust Soc Am.* **125** (1), 391-404 (2009).
45. Sidlof, P., Doaré, O., Cadot, O., & Chaigne, A. Measurement of flow separation in a human vocal folds model. *Exp Fluids.* **51** (1), 123-136 (2011).
46. Smith, S.L., & Thomson, S.L. Effect of inferior surface angle on the self-oscillation of a computational vocal fold model. *J Acoust Soc Am.* **131** (5), 4062-4075 (2012).
47. Khosla, S., Oren, L., Ying, J., & Gutmark, E. Direct simultaneous measurement of intraglottal geometry and velocity fields in excised larynges. *Laryngoscope.* **124** S1-S13 (2014).
48. Brücker, C., Kirmse, C., & Triep, M. Feedback of the glottal jet flow with supraglottal wall oscillations. *Acta Acustica United With Acustica.* **102** (2), 240-243 (2016).
49. Herbst, C.T., Fitch, W.T., Lohscheller, J., & Svec, J.G. Estimation of the vertical glottal shape based on empirical high-speed video and electroglottographic data. In: *AQL 2013, Proceedings of the 10th International Conference on Advances in Quantitative Laryngology, Voice and Speech Research, June 3-4, 2013, Cincinnati, Ohio, USA.* Deliyski, D.D. ed., AQL Press, Cincinnati, Ohio, 75-76 (2013).
50. Berke, G.S., & Gerratt, B.R. Laryngeal biomechanics: an overview of mucosal wave mechanics. *J Voice.* **7** (2), 123-128 (1993).
51. Boessenecker, A., Berry, D.A., Lohscheller, J., Eysholdt, U., & Doellinger, M. Mucosal wave properties of a human vocal fold. *Acta Acustica United With Acustica.* **93** (5), 815-823 (2007).
52. Hirano, M. *Clinical examination of voice.* Vol. 5, Springer-Verlag, Wien, Austria (1981).
53. Jing, B., Tang, S., Wu, L., Wang, S., & Wan, M. Visualizing the Vibration of Laryngeal Tissue during Phonation Using Ultrafast Plane Wave Ultrasonography. *Ultrasound in Med Biol.* **42** (12), 2812-2825 (2016).
54. Herbst, C.T. In: *Vertebrate Sound Production and Acoustic Communication.* Suthers, R.A., Fitch, W.T., Fay, R.R., & Popper, A.N. eds., Ch. 6, Springer International Publishing Switzerland, 159-189 (2016).